JOURNAL OF MATERIALS SCIENCE 35 (2000) 593–598

Surface characteristics of a porous-surfaced Ti-6Al-4V implant fabricated by electro-discharge-compaction

W. H. LEE, J. W. PARK
Department of Metallurgical Engineering, Hanyang University, Seoul 133-791, Korea

D. A. PULEO
Center for Biomedical Engineering, University of Kentucky, Lexington, KY 40506, USA

JUNG-YEUL KIM*
Department of Semiconductor Engineering, Uiduk University, Kyongju 780-713, Korea
E-mail: JYKIM@mail.uiduk.ac.kr.

Electro-discharge-compaction (EDC) is a unique method for producing porous-surfaced metallic implants. The objective of the present studies was to examine the surface characteristics of the Ti-6Al-4V implants formed by EDC. Porous-surfaced Ti-6Al-4V implants were produced by employing EDC using 480 μF capacitance and 1.5 kJ input energy. X-ray photoelectron spectroscopy was used to study the surface characteristics of the implant materials. C, O, and Ti were the main constituents, with smaller amounts of Al and V. EDC Ti-6Al-4V also contained N. Titanium was present mainly in the forms of mixed oxides and small amounts of nitride and carbide were observed. Al was present in the form of aluminum oxide, while V in the implant surface did not contribute to the formation of the surface oxide film. The surface of conventionally prepared Ti-6Al-4V primarily consists of TiO_2, whereas, the surface of the EDC-fabricated Ti-6Al-4V consists of complex Ti and Al oxides as well as small amounts of titanium carbide and nitride components. However, preliminary studies indicated that the implant was biocompatible and supports rapid osseointegration.

1. Introduction

Porous-surfaced implants have been developed to provide mechanical attachment of implants to tissue. Although the initial applications have been focused on the porous polymers and ceramics, porous metals are now commonly used in orthopedic and dental applications [1–3]. Of these, Ti and Ti-6Al-4V are often considered most suitable for high surface area implants.

Fabrication of porous-coated titanium and Ti-6Al-4V implants normally involves either plasma-spraying or sintering powders onto a solid substrate [4–6]. The high temperatures involved in these processes, however, resulted in detrimental changes in the microstructure and mechanical properties. In contrast, electro-discharge-compaction (EDC) allows fabrication of porous-surfaced implants without undesireable microstructural changes in the material [7]. EDC employs a high voltage, high current electrical pulse to consolidate powder particles. By manipulating the capacitance and input energy, the porosity and solid core size can be controlled. *In vivo* experiments using Ti-6Al-4V implants prepared by EDC have generally shown good results [7–9].

In addition to pore size and motion at the tissue-implant interface, the surface properties of the implant will affect tissue integration [10, 11]. Important surface characteristics of metallic biomaterials include composition and structure of the surface oxide and contamination of the surface [12–14]. Although surface properties of conventional Ti and Ti-6Al-4V implants have been frequently examined [15, 16], but the surface characteristics of EDC implants have not been reported. Because of the unique nature of the EDC process, it is necessary to investigate the surface characteristics of Ti alloy prepared by this method and compare the properties to those of a conventional Ti alloy system. Therefore, X-ray photoelectron spectroscopy (XPS) has been employed to examine the surface chemical composition of porous-surfaced Ti-6Al-4V implant prototype fabricated by EDC.

2. Materials and method

2.1. EDC Ti-6Al-4V

The ECD experimental set-up employed in this work has been described previously [7]. Atomized Ti-6Al-4V

* Author to whom all correspondence should be addressed.

powders, produced by the rotating electrode process (Goodfellow, Berwyn, PA), were sieved to yield one particle size class of 150–250 μm. One gram of powder was vibrated into a 3.3 mm I.D. Pyrex tube that had a copper electrode at the bottom. The resulting powder column was 41 mm high. A second copper electrode was placed on top, such that it contacted the powder column without exerting any external pressure other than the weight of the electrode. A capacitor bank (480 μF) was charged with electrical input energy (1.5 kJ), and a vacuum ion switch was evacuated to close the discharge circuit. The capacitor bank instantaneously discharged through the powder column, producing the Ti-6Al-4V implant with a solid core diameter (D_c) of 2.24 mm, resulting in 68% D_c/D_0, where D_0 is an implant diameter [7]. Discharge time and heat generated were about 300 μsec and 973 J, respectively. The average pore diameter was 121 μm, with a 45 μm average neck size between particles. The yield strength of the solid core was estimated about 755 MPa [7].

2.2. Surface analysis

EDC Ti-6Al-4V implant prototype was mounted on the spectrometer probe tip by means of double-sided adhesive tape and examined by XPS employing a Kratos XSAM 800 spectrometer with Mg K_α (1.25 keV) radiation. The system pressure was maintained below 5×10^{-9} torr using ion and Ti sublimation pumps to minimize contributions from vacuum contaminants. The spectrometer was run in constant pass energy mode at a pass energy of 12 kV and 14 mA. Under these conditions, the full width at half maximum (FWHM) of the Ag $3d_{5/2}$ peak was 1.1 eV, and the binding energy difference between Ag $3d_{5/2}$ and Ag $3d_{3/2}$ was 6.0 eV. The analyzer work function was determined by assuming the binding energy of the Ag $3d_{5/2}$ peak to be 368.2 eV. When the Ag $3d_{5/2}$ peak was used as the reference peak, the binding energy of the C 1s peak of adventitious carbon on the standard silver surface was 285 eV. All binding energies were referenced to the C 1s peak to correct for sample charging. Atomic concentrations were determined from the peak areas using the atomic sensitivity factors provided with the spectrometer. Ar^+ ion sputtering was carried out up to 10 minutes using a differentially pumped and computer-controlled 3M mini-beam ion gun. The ion gun was operated at 3.5 keV, and the sample current was kept at 9.3 mA. The pressure in the main chamber was kept at approximately 5×10^{-7} torr during Ar^+ ion sputtering. Under these conditions, the etching rate was approximately 25 Å/min, as determined from a SiO_2 standard film.

3. Results and discussion

Fig. 1 shows a typical XPS wide scan spectrum of the porous-surfaced Ti-6Al-4V implants over the binding energy ranges of 0–800 eV. The spectrum showed the major elements, carbon, oxygen, and titanium, as well as minor components, aluminum, vanadium, and nitrogen on the surface of the sample. Results of quantitative peak analyses are shown in Table I.

EDC Ti-6Al-4V implant prototype was further analyzed by employing Ar^+ ion sputtering followed by XPS measurements. Although different features such as preferential sputtering, atomic mixing, particle size effects, etc., can affect the etching profiles, similar etching rates of the Ti alloys were expected in the present studies [17, 18]. Ar^+ ion sputtering was carried out for up to 10 minutes. Surface elemental concentrations following Ar^+ ion sputtering are also given in Table I. Ar^+ ion sputtering decreased the amount of carbon, but the percentages of all other elements (O, Ti, Al, V, and N) increased. These results can be attributed to the removal of adventitious carbon with consequent exposure of the implant surface.

High resolution scans were then used to obtain information regarding the surface chemical state of the

TABLE I Surface chemical composition of the porous EDC Ti-6Al-4V sample before and after 10 min. of Ar^+ ion sputtering

	Concentration (At. %)	
Element	Before	After
C 1s	49.18	29.87
O 1s	19.55	27.19
Ti 2p	16.57	24.35
Al 2p	8.33	9.72
V 2p	1.85	2.64
N 2p	4.57	6.23

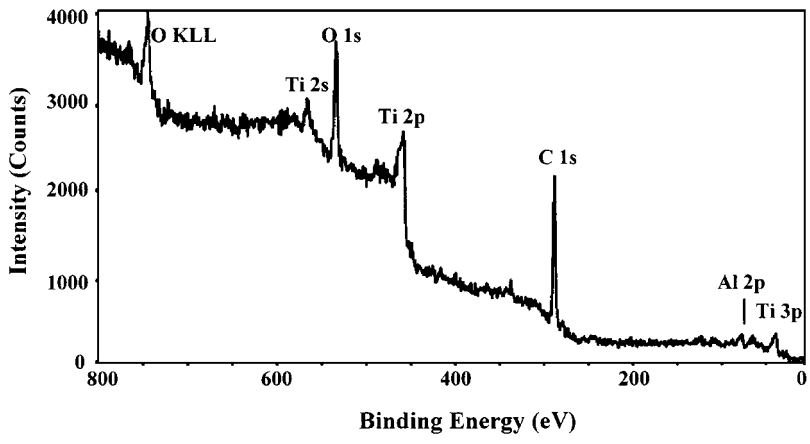

Figure 1 XPS survey spectrum of the porous-surfaced Ti-6Al-4V implant fabricated by EDC.

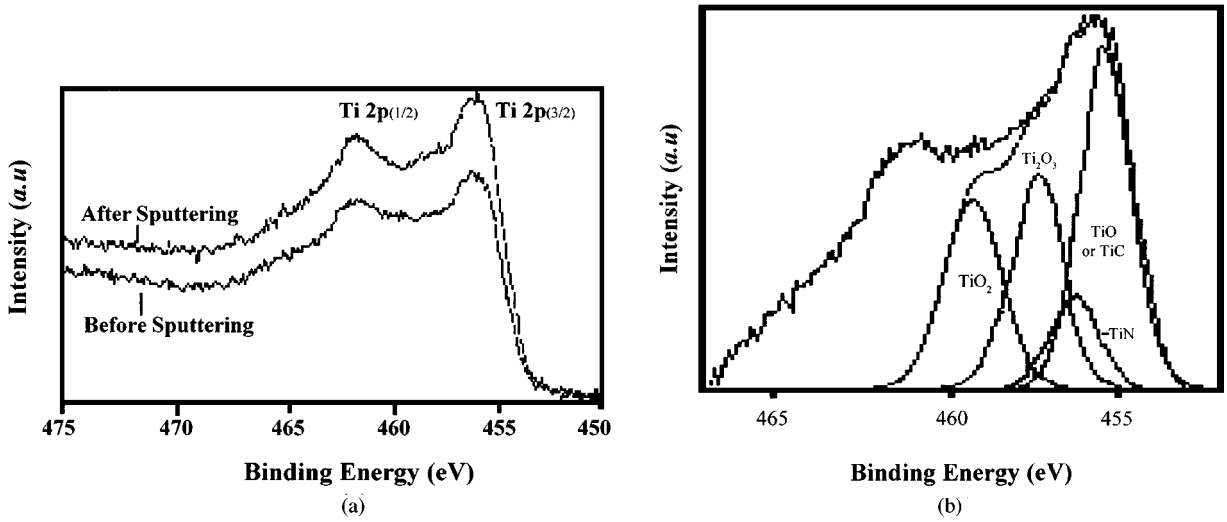

Figure 2 (a) XPS high resolution spectra of the Ti 2p region and (b) Deconvolution of Ti 2p peak to show contributions of four different functionalities.

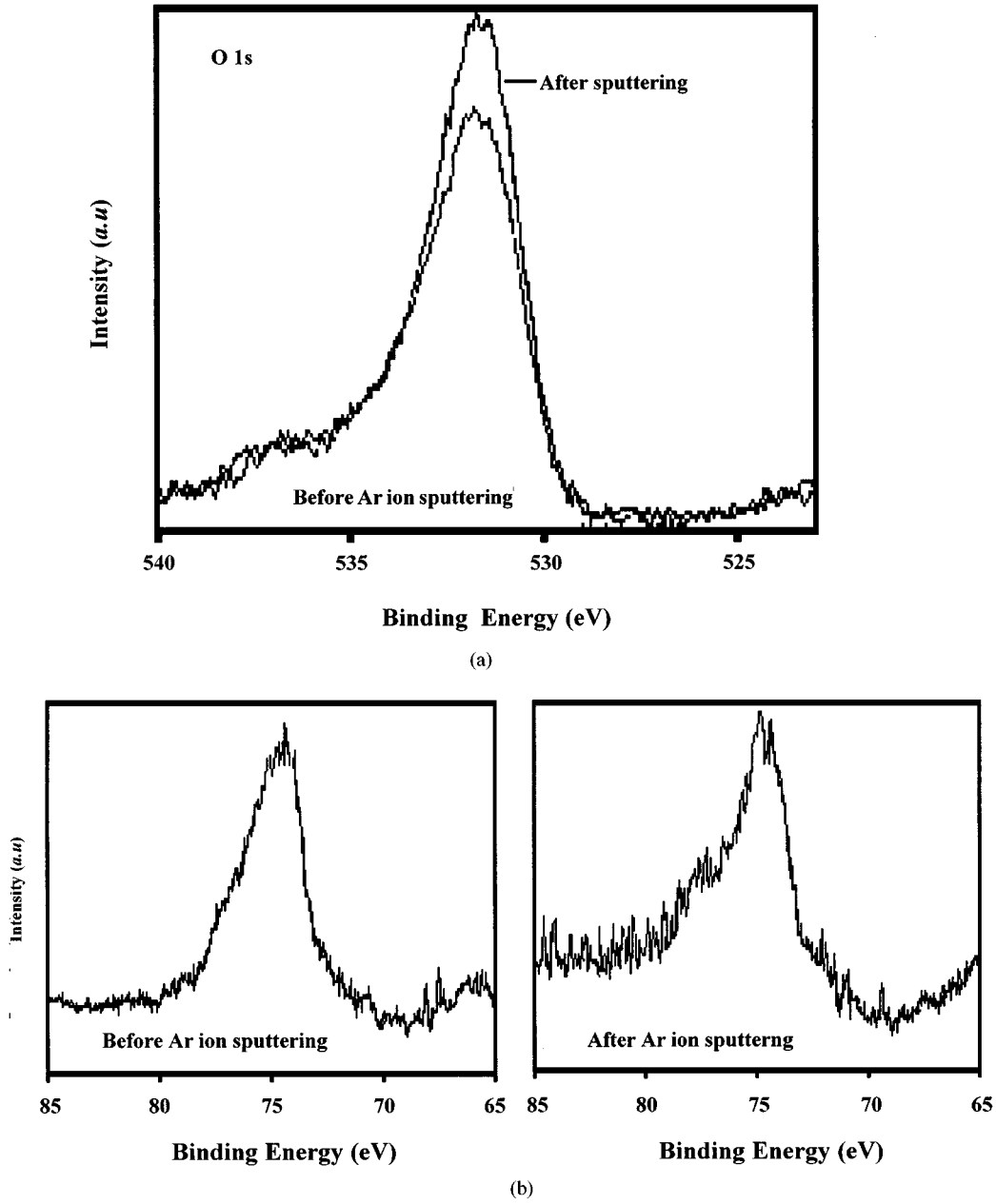

Figure 3 XPS high resolution spectra of the (a) O 1s region and (b) Al 2p region.

materials. Fig. 2(a) shows narrow scan spectra of the Ti 2p region. EDC Ti-6Al-4V showed a Ti $2p_{3/2}$ peak at 455.7 eV, with 5.6 eV splitting between the Ti $2p_{1/2}$ and Ti $2p_{3/2}$ peaks. Previous results on Ti narrow scan spectra of wrought Ti and Ti alloy show Ti $2p_{3/2}$ peak at about 459.2 eV with 5.8 eV splitting between the Ti $2p_{1/2}$ and Ti $2p_{3/2}$ [19–22]. For Ti^{4+}, as in TiO_2, the Ti $2p_{3/2}$ peak is at about 459.1 eV [17]. Thus, the surface of wrought Ti and Ti alloy is primarily in the form of TiO_2. However, in the case of EDC Ti-6Al-4V, high intensity regions between Ti $2p_{3/2}$ and Ti $2p_{1/2}$ peaks were observed. Peak shifts for Ti^{3+} (Ti_2O_3), Ti^{2+} (TiO), and Ti (metal) are approximately -1.7, -3.5, and -5.2 eV, respectively [20, 21]. For TiN, the Ti $2p_{3/2}$ peak is at about 456.2 eV [17]. The Ti $2p_{3/2}$ binding energy of 455.7 eV is similar to that of Ti 2p for TiO and TiC. The presence of TiC and TiN on EDC Ti-6Al-4V surfaces is supported by observation of a shoulder region at about 282.5 eV in the C 1s narrow spectrum and by the binding energy of N 1s for nitride, respectively. The narrow scan spectra of C 1s and N 1s will be discussed later. The Ti 2p peak was deconvoluted using a peak synthesis procedure that fits the measured peak to several Gaussian peaks. A typical deconvoluted XPS high resolution Ti 2p spectrum is shown in Fig. 2b. It was found that the Ti 2p peak could be fitted to four major line shapes with peak binding energies of 455.5, 456.2, 457.4, and 459.2 eV. These peaks were assigned to TiO/TiC, TiN, Ti_2O_3, and TiO_2, respectively. High current density results in rearrangement of oxide because of movement of Ti and O ions [20, 22]. This result can be ascribed to EDC breaking the oxide film of metal powder during the discharge process [23].

High resolution spectrum of the O 1s region for EDC Ti-6Al-4V is shown in Fig. 3a. The O 1s peak had a maximum at 531.9 eV with FWHM of 2.79 eV. The asymmetry on the high B.E. region and broadness of this peak are generally interpreted as indicating

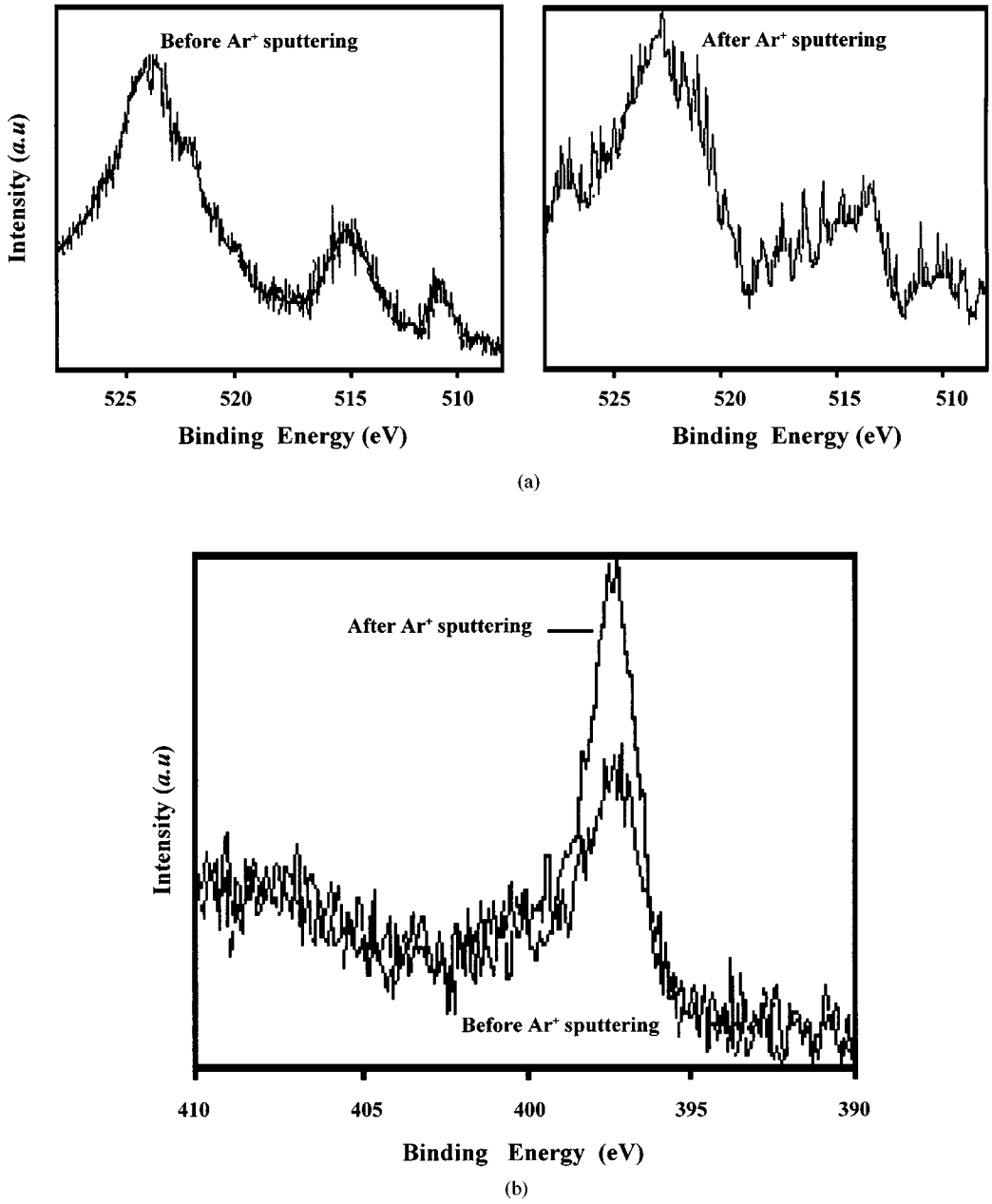

Figure 4 XPS high resolution spectra of the (a) V 2p region and (b) N 1s region.

hydrated metal oxide [20, 24]. Considering the results for the Ti 2p peak, however, the asymetry of the O 1s peak could indicate complex overlapping oxides.

Narrow scan spectrum of the Al 2p region is shown in Fig. 3b. The maximum was positioned at about 75 eV. This is about 2 eV higher value than the binding energy of elemental Al (metal). The B.E. shift can be attributed to oxidation of Al producing such as Al_2O_3. Therefore, the EDC Ti-6Al-4V surface contains aluminum oxide in addition to titanium oxide. The presence of Al in the surface oxide of the titanium alloy has also been previously reported [19].

Representative high resolution spectrum of the V 2p region is shown in Fig. 4a. This spectrum shows a V $2p_{3/2}$ peak at 513.5 eV, with 7.6 eV splitting between the V $2p_{1/2}$ and V $2p_{3/2}$ peaks. Because the peak position for vanadium oxide is at 516.5 eV [25], the spectrum indicates that V is not coordinated with O in the EDC Ti-6Al-4V. Thus, the small amount of V detected in the EDC Ti-6Al-4V surface did not contribute to the formation of the surface oxide film. Similar results for the wrought Ti-6Al-4V were reported by Hanawa and Ota [26]; however, Ask [19] did not detect V in the oxide.

Fig. 4b shows a representative high resolution spectrum of the N 1s region. The maximum at 397.2 eV is identical to the N 1s position for nitride. This indicates the presence of a small amount of nitride and supports assignment of a TiN peak to the Ti 2p spectrum in Fig. 2a. The formation of nitride can be explained by the electrical discharge in air resulting in reaction between nitrogen and the titanium substrate.

Adventitious carbon, attributable to exposure to air, is normally detected on the surface of Ti and Ti-6Al-4V [26, 27]. An asymmetric peak with a maximum at 285 eV was observed. This maximum represents carbon in the C–H form. Although the maximum appeared at 285 eV, the C 1s peak also contained high and low binding energy components, which indicate the presence of additional carbon-based surface functional groups.

To elucidate the additional functionalities, the C 1s peak was also deconvoluted using a peak synthesis procedure that fits the measured peak to several Gaussian peaks, each with an average FWHM value of 2 eV and a fixed binding energy [25, 28–31]. To obtain the best fit between the experimental and the synthesized spectra, the intensity contribution of each functional component peak was estimated by a computer simulation. A typical XPS high resolution C 1s spectrum deconvoluted into surface functional group contributions is shown in Fig. 5. It was found that, in addition to a peak centered at 285 eV (C─H), the carbon 1s peak could be fitted to four line shapes with peak binding energies of 282.5, 286.7, 287.7, and 289.9 eV. These peaks were assigned to carbide, alcohol or ester (C─O), carbonyl (C=O), and carboxyl (O─C=O) functionalities, respectively [24]. As shown in Table II, the contributions of the different functionalities to the total area of the C 1s peak region of the EDC Ti-6Al-4V were: 6.9% carbide, 58.7% C─H, 22.4% C─O, 8.6% C=O, and 3.1% O─C=O. Oxidized carbons in adsorbed contaminant overlayers are not surprising. Interestingly, and

TABLE II Carbon functional components on EDC Ti-6Al-4V obtained from deconvolution of the C 1s peak before and after 10 min. of Ar^+ ion sputtering

	Contribution to total peak area (%)	
Functional group	Before	After
C─Ti	6.9	12.9
C─H	58.7	59.0
C─O	22.4	18.3
C=O	8.6	5.9
O─C=O	3.1	2.9

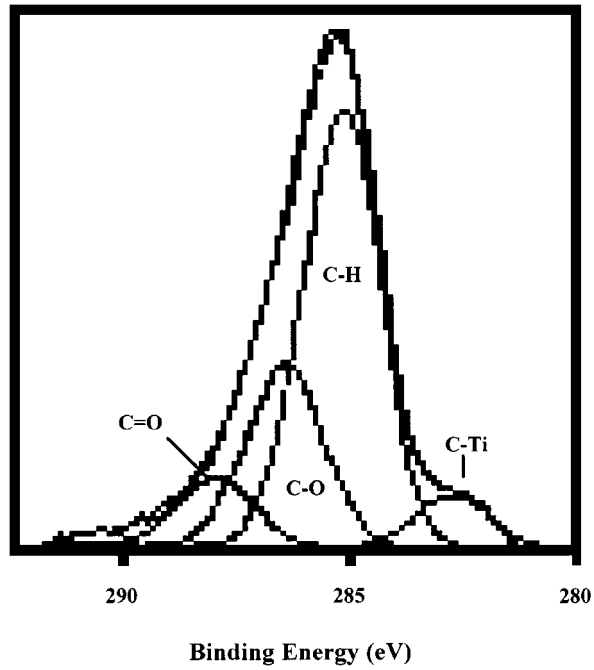

Figure 5 Deconvolution of C 1s peak to show contributions of four different functionalities.

in contrast to wrought Ti-6Al-4V, the EDC process resulted in the formation of a small amount of titanium carbide. Formation of TiC can be attributed to the high heat generated on the surface of the Ti-6Al-4V powder during discharge which induced the reaction between Ti and C.

Table II also contains the calculated contribution of the different carbon peak components after 10 min of Ar^+ ion sputtering. Although the functionalities were the same as those identified before sputtering, changes in the relative proportions were observed. The oxidized carbon components decreased and the carbide component increased following sputtering, while the percentage of C─H did not change. These observation can be attributed to removal of contaminant carbon overlayers with subsequent exposure of TiC.

4. Conclusion

EDC is a unique method for fabricating porous-surfaced implants. The present studies show that the surface chemistry of EDC implant prototype differs from that of conventional wrought Ti-6Al-4V. Whereas EDC Ti-6Al-4V surfaces are mainly composed of mixed Ti oxide and small amounts of Ti nitride and

Ti carbide, the surface of wrought Ti-6Al-4V is mainly in the form of TiO_2. Preliminary studies, however, indicate that the implants are biocompatible and support rapid osseointegration.

References

1. D. F. WILLIAMS, "Biocompatibility of Orthopedic Implants" (CRC Press, Boca Raton, 1982) p. 49.
2. M. SPECTOR, in "Biocompatibility of Orthopedic Implants," edited by D. F. Williams (CRC Press, Boca Raton, 1982) p. 55.
3. *Idem., ibid.* edited by D. F. Williams (CRC Press, Boca Raton, 1982) p. 89.
4. K. ASAOKA, N. KUWAYAMA, O. OKUNO and I. MIURA, *J. Biomed. Mater. Res.* **19** (1985) 699.
5. S. YUE, R. M. PILLAR and G. C. WEATHERLY, *ibid.* **18** (1984) 1043.
6. R. M. PILLIAR, *ibid.* **21** (1987) 1.
7. K. OKAZAKI, W. H. LEE, D. K. KIM and R. A. KOPCZYK, *ibid.* **25** (1991) 1417.
8. J. T. DOMINICI, P. J. SAMMON, J. F. DRUMMOND, M. I. LIFLAND, R. GEISSLER and K. OKAZAKI, *J. Oral Implantol.* **20** (1994) 299.
9. J. F. DRUMMOND, J. T. DOMINICI, P. J. SAMMON, K. OKAZAKI, R. GEISSLER, M. I. LIFLAND, S. A. ANDERSON and W. RENSHAW, *ibid.* **21** (1995) 295.
10. B. KASEMO, *J. Prosth. Dent.* **49** (1983) 832.
11. B. KASEMO, J. LAUSMAA, P. I. BRANERMARK, G. A. ZARB and T. ALBREKTSSON, in "Tissue -Integrated Prostheseses" (Quintessence Books, Chicago, 1985) p. 137.
12. K. GOMI and J. E. DAVIES, *J. Biomed. Mater. Res.* **27** (1993) 429.
13. J. Y. MARTIN, Z. SCHWARTZ, T. W. HUMMERT, D. M. SCHRAUB, J. SIMPSON, J. LAUKFORD, D. D. DEAN, D. L. COCHRAN and B. D. BOYAN, *ibid.* **29** (1995) 389.
14. B. GROESSNER-SCHREIBER and R. S. TUAN, *J. Cell Sci.* **101** (1992) 209.
15. J. L. ONG, C. W. PRINCE and L. C. LUCAS, *J. Biomed. Mater. Res.* **29** (1995) 165.
16. E. LEITAO, M. BARBOSA and K. DE GROOT, *J. Mater. Sci.: Mater. Med.* **8** (1997) 423.
17. J. Y. KIM, P. J. REUCROFT, V. R. PRADHAN and I. WENDER, *Fuel Proc. Technol.* **34** (1993) 207.
18. J. Y. KIM, P. J. REUCROFT, M. TAGHIEI, V. R. PRADHAN and I. WENDER, *Energy and Fuels* **8** (1994) 886.
19. M. ASK, J. LAUSMAA and B. KASEMO, *Appl. Surf. Sci.* **35** (1989) 283.
20. N. R. ARMSTRONG and R. K. QUINN, *Surf. Sci.* **67** (1977) 451.
21. W. GOPEL, J. A. ANDERSON, D. FRANKEL, M. JAEHNIG, K. PHILLIPS, J. A. SHAFFER and G. ROCKER, *ibid.* **139** (1984) 333.
22. C. N. SAYERS and N. R. ARMSTRONG, *ibid.* **77** (1978) 301.
23. D. K. KIM, H. R. PAK and K. OKAZAKI, *Mat. Sci. Eng.* **A104** (1988) 191.
24. G. W. SIMMONS and B. C. BEARD, *J. Phys. Chem.* **91** (1987) 1143.
25. J. MOULDER, W. STICKLE, P. SOBAL and K. BOMBER, "Handbook of X-ray Photoelectron Spectroscopy" (Perkin Elmer Corp., Eden Prairie, 1992) p. 213.
26. T. HANAWA and M. OTA, *Appl. Surface Sci.* **55** (1992) 269.
27. *Idem., Biomaterials* **12** (1991) 767.
28. Q. WENMING, Q. ZHU and L. LING, in Extended Abstracts 22th Biennial Conference on Carbon (San Diego, July 1995) p. 400.
29. I. SILVA and L. RADORIC, in Extended Abstracts 22th Biennial Conference on Carbon (San Diego, July 1995) p. 444.
30. N. KORTYUKHORA, E. BUZOHEVA and A. SENKEVICH, *Carbon* **36** (1998) 549.
31. A. PUZIY and O. PODDBNAYA, *ibid.* **36** (1998) 45.
32. D. A. PULEO, *J. Biomed. Mater. Res.* **29** (1995) 951.
33. L. J. HOLT and D. A. PULEO, *Art. Cells Blood Subs. Immob. Biotech.* **24** (1996) 613.

Received 10 February
and accepted 22 July 1999